Mathematical Biosciences and Engineering

http://www.aimspress.com/journal/MBE

MBE, 16(5): 4546–4558
DOI: 10.3934/mbe.2019227
Received: 17 February 2019
Accepted: 26 April 2019
Published: 23 May 2019

Research article

Quantitative analysis of non-alcoholic fatty liver in rats via combining multiple ultrasound parameters

Yuanyuan Shen[1], Yuncheng Xing[1], Haoming Lin[1], Siping Chen[1], Baiying Lei[1,*], Jianhua Zhou[2], Zhong Liu[1] and Xin Chen[1,*]

[1] School of Biomedical Engineering, Shenzhen University, National-Regional Key Technology Engineering Laboratory for Medical Ultrasound, Guangdong Key Laboratory for Biomedical Measurements and Ultrasound Imaging, Shenzhen, Guangdong, P. R. China

[2] Department of Ultrasound, Sun Yat-Sen University Cancer Center, State Key Laboratory of Oncology in South China, Collaborative Innovation Center for Cancer Medicine, 651 Dongfeng Road East, Guangzhou, 510060, P. R. China

* **Correspondence:** Email: leiby@szu.edu.cn, chenxin@szu.edu.cn.

Abstract: Nonalcoholic fatty liver disease (NAFLD) is the most common chronic liver disease. The noninvasive and accurate classification of NAFLD is still a challenging problem. In this study we proposed a new quantitative ultrasound (QUS) technique, which combined multiple QUS parameters for distinguishing steatosis stages. NAFLD was induced in the livers of 57 rats by gavage feeding with a high fat emulsion, while 8 rats were given a standard diet to serve as controls. Ex vivo ultrasound measurement was conducted for capturing the radiofrequency signal. Six QUS parameters were extracted and selected for linear combination. The results show that the overall performance of the combined parameter is better than that of the single QUS parameter. The accuracy, sensitivity, specificity, and area under the receiver operating characteristic curve (AUROC) while using our proposed method to distinguish mild steatosis (stage S1) from the steatosis under stage S0 are 90.1%, 0.93, 0.88 and 0.97 respectively. In conclusion, the proposed method in this study can make up for the deficiency of single parameter and improve the quantitative staging ability of fatty liver, and thus could play an important role in the diagnosis of NAFLD.

Keywords: NAFLD; characteristic parameters; fusion; steatosis stage; quantitative analysis

1. Introduction

Non-alcoholic fatty liver disease (NAFLD) is a multi-system disease that not only causes liver function damage, but also affects other organs [1, 2]. For example, patients with NAFLD have a higher

mortality rate of liver disease and non-liver disease than ordinary people [3]. Therefore, the accurate assessment of the severity of NAFLD is critical for the prevention, diagnosis and treatment of fatty liver-related diseases. The pathologic definition of NAFLD is that more than 5% of liver hepatocytes have macro steatosis. NAFLD represents a spectrum of diseases ranging from simple steatosis to nonalcoholic steatohepatitis, which can progress to liver fibrosis, cirrhosis, and hepatocellular carcinoma [4].

Even though liver biopsy is considered as the gold standard for NAFLD diagnosis, it has inherent disadvantages such as invasiveness, complications, and being subjective [5, 6]. Conventional medical imaging methods for NAFLD diagnosis include computed tomography (CT), magnetic resonance imaging (MRI) and ultrasonography (US) [7, 8, 9, 10]. Among these modalities, US is the most commonly used method for NAFLD diagnosis because it is non-invasive, non-radiative, real-time, and inexpensive. It is suitable for people of all ages, including pregnant women and children, and is not limited by medical history [11]. Conventional ultrasound imaging is a semi-quantitative assessment. Therefore, it is subjective and relies on the experience of the operator [12]. However, quantitative ultrasound (QUS) imaging can provide specific tissue features and increase the specificity of conventional US. It has been widely applied in the liver fat quantification [13, 14].

Envelope statistics and spectral-based techniques are two major categories of QUS technique. Both of them have demonstrated success in NAFLD applications, providing additional diagnostic capabilities [13]. The envelope statistics technique utilized the shape and attributes of the envelope of the backscattered ultrasound to estimate the information about the underlying tissue microstructures. Various models and their derivations for the statistics of the envelope, such as the Nakagami model, the Rayleigh model, and the homodyned-K model, have been proposed over the past few decades for the biomedical ultrasound applications [15]. For the NAFLD diagnosis, the Nakagami model is currently the most frequently used one [16, 17, 18].

Spectral-based techniques include the estimation of attenuation coefficient (AC) and its derivatives, the estimation of backscatter coefficient (BSC) and its derivatives such as the effective scatterer diameter (ESD) and the effective acoustic concentration (EAC) of scatterers. These techniques utilize the amplitude, frequency and phase information in the ultrasonic RF signal and also have the ability to observe tissue microstructures. Paige *et al.* explored the diagnostic performance of AC and BSC for predicting histology-confirmed steatosis grade in NAFLD patients. Their results suggested that QUS parameters may be more accurate and provide higher interobserver agreement than CUS [19]. Yang *et al.* used the integral backscatter coefficient to evaluate the liver fat concentration after liver transplantation, and observed that the integrated backscatter coefficient (IBC) has a good correlation with liver fat concentration [17]. Lin *et al.* investigated the QUS measurements of BSC identify steatosis in animal models and found that BSC can accurately diagnose and quantify hepatic steatosis [21]. Ghoshal *et al.* studied ESD and EAC and the results indicated that the two parameters are sensitive to fat content in the liver [22].

The primary purpose of this study is to combine multiple QUS parameters using an efficient fusion method to obtain an optimal characteristic parameter. We identified six commonly used QUS parameters to measure different liver fat concentrations, and selected several parameters with better staging effects for combination. The diagnosis performance of the combined parameter was evaluated and compared with that of the single QUS parameter. To the best of our knowledge, this is the first study to combine multiple QUS parameters for evaluating liver steatosis grade.

2. Methods and materials

2.1. Animal model

The NAFLD rat model was supplied by the Guangdong Experimental Animal Center. The animal experiment obtained the review of the Experimental Animal Ethics Committee of Shenzhen University. The experimental rat weighed between 180 and 200 g. The culture environment of the experimental rat model was sterile and constant, the temperature and humidity of culture environment were maintained at $20-60^{\circ}$ and $40-70\%$, respectively. A total of 65 rats were involved in the study. The rats were randomly divided into the control group (8 rats) and the fatty liver group (57 rats). The rats in the control group were fed with a standard diet with sterilized food and water, while for those in the fatty liver group a high fat emulsion (20% lard, 10% cholesterol, 20% sodiumcholate, 0.5% propylthiouracil, and 30% fructose) was given once a day at 1 mL/100 g rat weight, for different numbers of days to induce different severity stages of steatosis. After 2, 4, 6, and 8 weeks, the rats were humanely killed for analysis. Specifically, the right lateral lobe of the liver was used for QUS measurements, while the rest lobes were for histologic assessment. It should be noted that the steatosis grade was ultimately determined by the histologic assessment, rather than the length of feeding time of the rats. Moreover, all procedures conducted in our study had been approved by the Animal Care Committee of Shenzhen University and the Guangdong Medical Laboratory Animal Center.

2.2. Histological assessment

Excised liver tissues were fixed in 10% formalin solution for at least 24 h. After washing and dehydrating, samples were embedded in paraffin and sliced to a thickness of 7 μm. The paraffin slices were stained with hematoxylin-eosin (HE) by histopathology technicians, and analyzed using a microscope (BX41, Olympus, Pittsburgh, PA) by an expert pathologist. According to the percentage of hepatocytes containing macrovesicular fat droplets, the severity grades for steatosis were defined as follows [23]: $S0 < 5\%$, $S1 = 5\% - 33\%$, $S2 = 33 - 66\%$, and $S3 \geq 67\%$. For an illustration, example sliced images for liver tissue sections with different steatosis stages are shown in Figure 1, where (a), (b), (c), and (d) represent normal liver, mild fatty liver, moderate fatty liver and severe fatty liver, respectively. It can be seen that hepatocytes containing macrovesicular fat droplets are increasing from (a) to (d) in the figure. The percent of hepatocytes containing macrovesicular fat droplets serves as the quantitative measurement for the determination of steatosis stage.

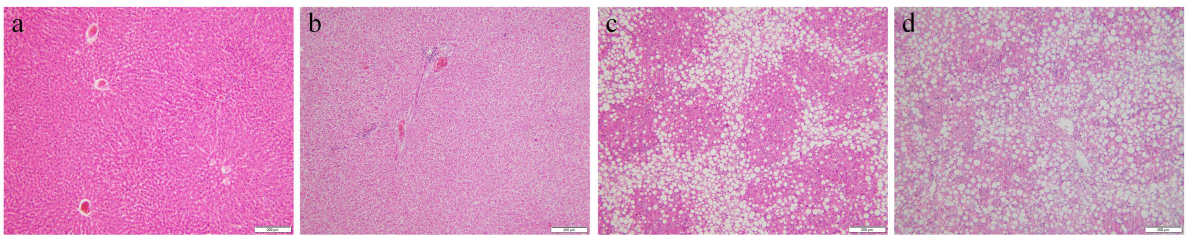

Figure 1. Example sliced images of isolated liver tissue under different steatosis stages: (a), (b), (c), and (d) are for normal liver, mild fatty liver, moderate fatty liver and severe fatty liver, respectively.

2.3. Ultrasound measurement

In an ex vivo experiment, the right liver lobe was processed and embedded in a fabricated gelatin phantom (gelatin from porcine skin, G2500, Sigma-Aldrich, St. Louis, MO, USA) in a container ($11 \times 11 \times 7$ cm). The objective for such design was to simulate the tissues that lie between the ultrasound probe and liver in vivo. A modified ultrasound scanner (M5, Mindray, Guangdong, China) with a linear array probe (7L4S) was used to capture the RF data. The center frequency of the probe is 7.5 MHz and the sampling frequency is 30 MHz. Each rat liver tissue phantom was scanned ten times and the ultrasound images and the corresponding RF data were stored for offline processing.

2.4. QUS parameter estimations

The ultrasound image was reconstructed from the corresponding RF data. Then the region of interest (ROI) is selected in the reconstructed image as shown in Figure 2. Six different QUS parameters were calculated based on the ROI which was divided into several sub-ROIs according to different algorithms. Here we just briefly introduce their definitions.

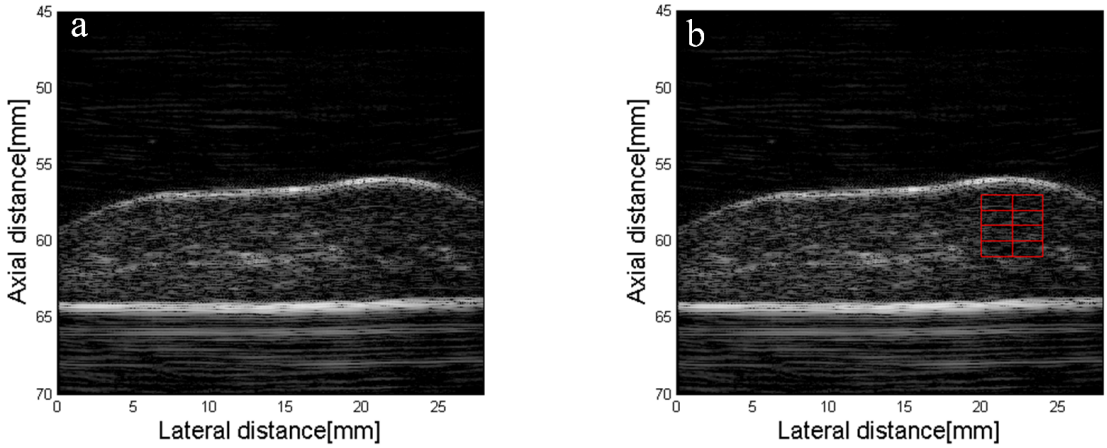

Figure 2. Selection of ROI area in ultrasound B images and ultrasound B images of isolated rat liver: the image area covered by the red grid indicates the region of interest (ROI) consisting of eight sub regions, from which the QUS parameters (LC values for the sub regions) obtained by using the proposed method are averaged for analysis.

2.5. Nakagami statistical parameters

We used the Nakagami statistical model to analyze the envelope and estimate the shape parameter m and the scaling parameter U [24]. The envelope of the RF signal was calculated by the Hilbert transform. The typical relationship between the RF signal and envelope waveform is shown in Figure 3. The probability density function (pdf) of the envelope signal x, which can be approximated as a Nakagami model with two parameters (m, U) as follows:

$$f(x) = \frac{2m^m}{\tau(m)u^m} x^{2m-1} \exp(-\frac{m}{u}x^2), \tag{2.1}$$

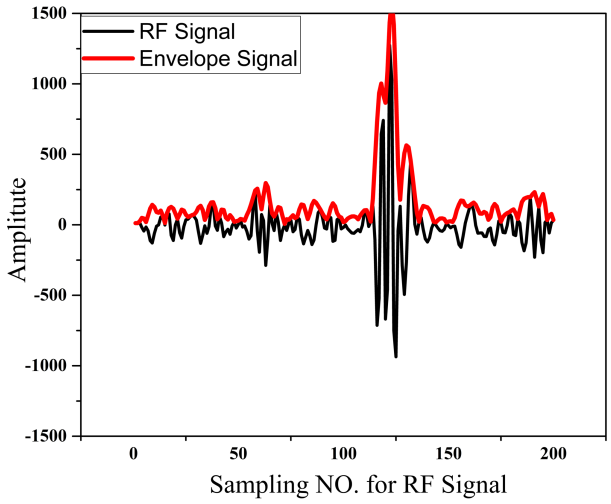

Figure 3. Ultrasonic RF signal and its corresponding envelope information.

where $\tau(\cdot)$ is the gamma function, the parameters m and U are represented as:

$$\triangle = \ln\left(E\left(\sum_{i=1}^{i=N} x_i^2\right)\right) - \frac{1}{N}\sum_{i=1}^{i=N} \ln\left(x_i^2\right), \tag{2.2}$$

$$m_{MLE} = \begin{cases} \dfrac{0.5001 + 0.1649\triangle - 0.0544\triangle^2}{\triangle}, & \text{if } 0 < \triangle < 0.5772, \\ \dfrac{8.8989 + 9.0600\triangle + 0.9755\triangle^2}{\triangle(17.7973 + 11.9685\triangle + \triangle^2)}, & \text{if } 0.5772 < \triangle < 17, \end{cases} \tag{2.3}$$

$$U = \log\left(E\left(x^2\right)\right). \tag{2.4}$$

2.6. Attenuation coefficient slope (ACS)

The attenuation coefficient slope as a function of frequency is expressed in dB/MHz/cm and is obtained by the following equation [25]:

$$\frac{\ln\left(S\left(f, Z_1\right)\right) - \ln\left(S\left(f, Z_2\right)\right)}{4d} + \beta_r f = \beta_s f, \tag{2.5}$$

where $S(f, Z_1)$ denotes the power spectrum at depth Z_1, $S(f, Z_2)$ denotes the power spectrum at depth Z_2, f is the frequency, d denotes the distance between Z_1 and Z_2, $d = Z_2 - Z_1$, Z_1 and Z_2 are the distance from the probe to the ROI (in cm). β_r and β_s denote ACS of reference phantom and tissue (dB/MHz/cm), respectively. We also normalized the power spectrum by dividing the measured power spectrum by the standard power spectrum, which is denoted as

$$S(f, Z) = \frac{S_s(f, Z)}{S_r(f, Z)}, \tag{2.6}$$

where $S_s(f, Z)$ denotes the measured power spectrum, $S_r(f, Z)$ denotes the reference power spectrum, Z is depth.

2.7. Integrate backscatter coefficient (IBC)

The integrate Backscatter coefficient, expressed in dB, is estimated using [22]:

$$IBC = \frac{1}{f_{min} - f_{max}} \int_{f_{min}}^{f_{max}} BSC(f)df, \tag{2.7}$$

where $BSC(f)$ is the ultrasonic backscatter coefficient, which is estimated in accordance with the method described by [26]:

$$BSC = 10\log_{10}\left[\frac{S_s(f,Z)}{S_r(f,Z)}\exp(4\beta_r Z)\frac{1}{0.63^2}\frac{R_p^2 k^2 a^2}{8\Omega l\left[1+\left(\frac{ka^2}{4F}\right)^2\right]}\right], \tag{2.8}$$

where R_p is the reflection coefficient from the plane reflector (assumed to be one), k is the wave vector, a is the transducer radius, F is the transducer focal distance, l is the thickness of segmentation window.

2.8. Effective scatterer diameter (ESD) and effective acoustic concentration (EAC)

From a microscopic point of view, the backscattered theoretical power spectrum can also be expressed as [27]:

$$W_{thero}(f) = \frac{185lq^2a_{eff}^6 f^4 pz_{var}^2}{1+2.66\left(fqa_{eff}\right)^2}e^{-(3.487fa_{eff})^2}, \tag{2.9}$$

where f is the frequency (MHz), a_{eff} denote the effective scatterer diameter (ESD) (mm), p is the scatterer concentration (mm^{-3}), $z_{var} = \frac{z-z_0}{z_0}$ is relative acoustic impedance of the scatterer and its surrounding medium, pz_{var}^2 denote the effective acoustic concentration (EAC), l is the window length (mm), q is the transducer aperture.

The power spectrum is linearly fitted in the bandwidth by the least squares fitting method based on frequency f. The spectral slope and the intermediate frequency amplitude are m_s and M, respectively. The effective scatter diameter (ESD) and effective acoustic concentration (EAC) are obtained by the following equation, respectively:

$$ESD = \sqrt{\frac{g_3(f_c,b)n - m_s}{g_4(f_c)}}, \tag{2.10}$$

$$EAC = \frac{exp\left(\frac{M-4.34\ln E - g_1(f_c,b)n - g_2(f_c)a_{eff}^2}{4.34}\right)}{a_{eff}^{2(n-1)}}, \tag{2.11}$$

where g_1, g_2, g_3, g_4 are constants, b is the fractional bandwidth, E is a constant related to the aperture and focal length, and n is set as 4 for the biological tissue are isotropic scatterers.

2.9. Combination of multiple QUS parameters

To select the appropriate parameters for predicting NAFLD, a univariate analysis was performed on the parameters mentioned above. Four parameters (m, U, IBC, EAC) showed as the most significant

predictors for the NAFLD stage. These four parameters were then used for construct a combination model. An optimal linear combination of the four parameters was used to improve the prediction of mild steatosis (stage ≥ S1). The method proposed by [28, 29] was used to determine the optimal linear combination which has the greatest AUROC out of all the possible linear combinations. The combination coefficients and corresponding cut-off values were calculated. Comparisons of the performances between the single parameters and their linear combination were performed.

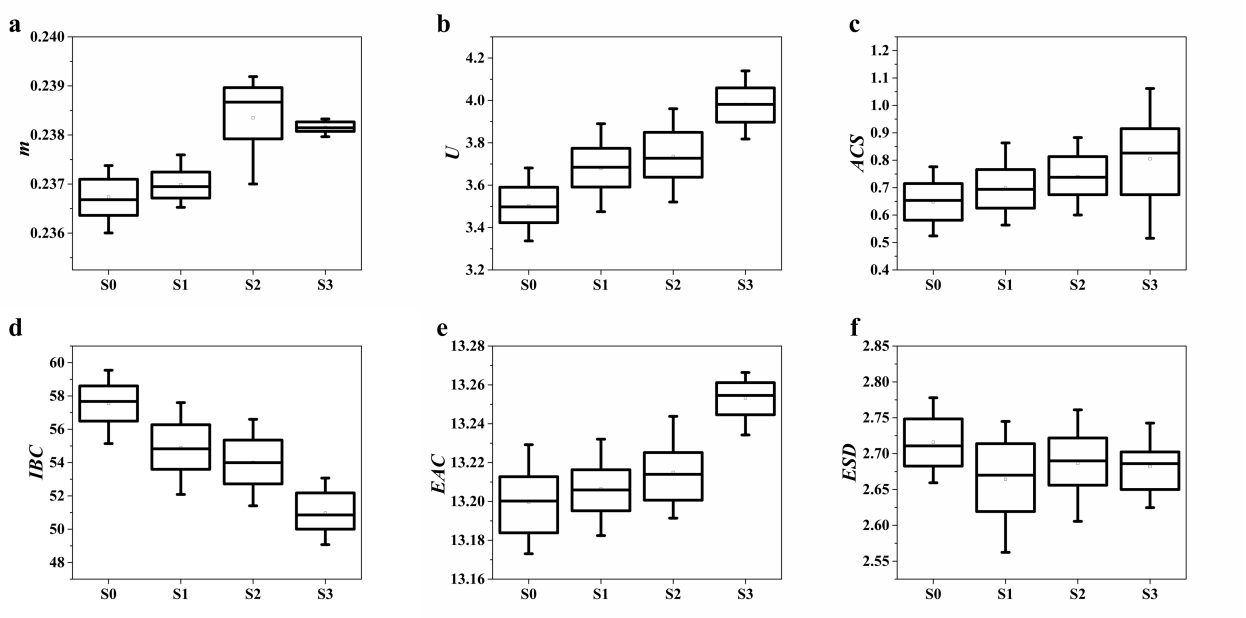

Figure 4. Distribution of six characteristic parameters at different hepatic fat concentrations. Subfigures from (a) to (f) are box plots of different quantitative parameters respectively for the shape parameter m and the scaling parameter U, the attenuation coefficient slope (ACS), the integrated backscattering coefficient (IBS), the effective acoustic concentration (EAC) and the effective scatterer diameter (ESD). In each subfigure, middle bar represents the median value for the parameter across different rat samples, bottom and top of the box represent the 25th and 75th percentiles, respectively, and the whiskers represent the minimum and maximum values. It can be clearly observed that the parameter m, U, IBC, EAC are well correlated with the NAFLD stages (S0, S1, S2, S3).

3. Results

The box plots of the six QUS parameters for different NAFLD stages are shown in Figure 4. In this figure we can clearly observe that the parameter m, U, IBC, EAC are well correlated with the NAFLD stages. The formula of the optimal linear combination was

$$LC = 5 \times U + m - 1.8 \times IBC + 0.3 \times EAC. \tag{3.1}$$

As mentioned earlier, the coefficients in the equation were determined by using the method reported in [28, 29], which explores the information carried by the marker values in different testing groups and

Table 1. Classification Performances of QUS Parameters and the Combined Parameter.

	Parameters	*m*	*U*	*IBC*	*EAC*	Combination
	AUC	0.790	0.898	0.926	0.701	0.970
stage ≥ S1	ACC	0.726	0.804	0.825	0.655	0.901
	Sen	0.467	0.647	0.724	0.933	0.938
	Spe	1.0	0.966	0.945	0.378	0.877
	AUC	0.953	0.817	0.841	0.777	0.933
stage ≥ S2	ACC	0.916	0.718	0.703	0.720	0.894
	Sen	0.835	0.576	0.718	0.447	0.894
	Spe	0.835	0.880	0.772	0.861	0.897
	AUC	0.857	0.976	0.972	0.996	0.933
stage = S3	ACC	0.814	0.936	0.932	0.967	0.976
	Sen	1.0	1.0	1.0	1.0	1.0
	Spe	0.84	0.854	0.855	0.971	0.963

employs the Fishers linear discriminant function for the optimization. The resultant linear combination provided us the maximum value of AUROC for better steatosis assessment. The box plot of the combined parameter for different NAFLD stages is shown in Figure 5. The performance of the combined parameter was analyzed and compared with those of the single parameter. The ROC curves of the six QUS parameters and the combined parameters for differentiating NAFLD stages are shown in Figures 6 and 7, respectively. The performance of different parameters are listed in Table 1.

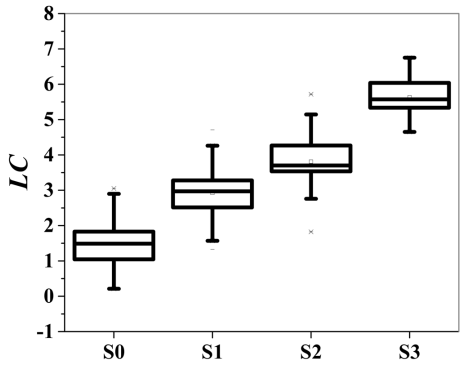

Figure 5. Box plot of the combined parameters at different hepatic fat concentrations.

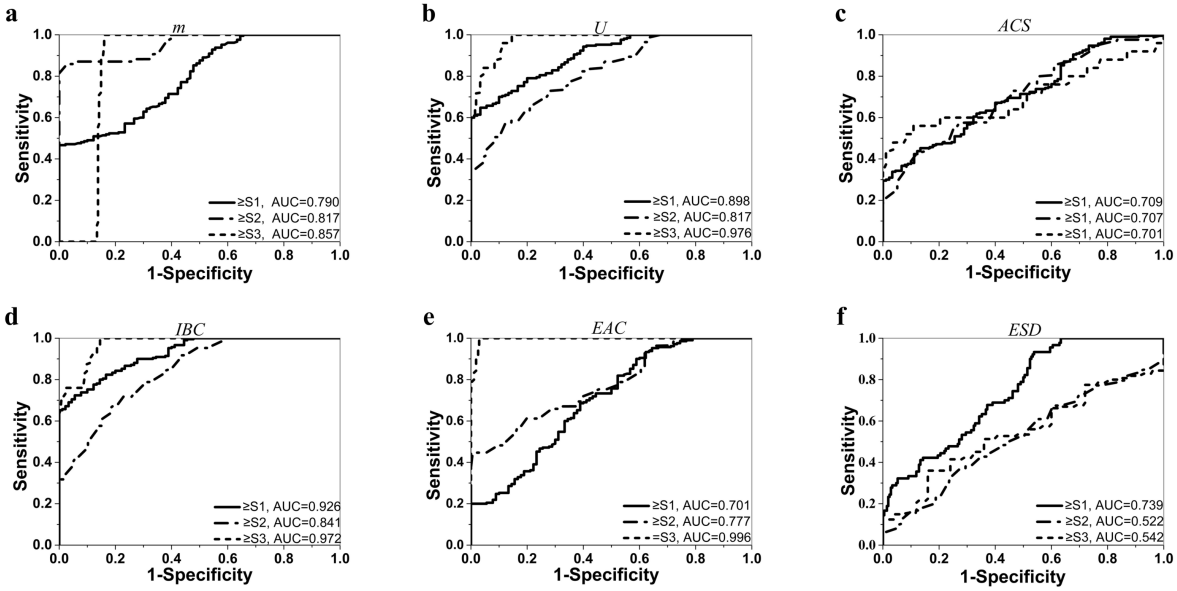

Figure 6. ROC curve and AUC values for different liver fat concentrations for the six characteristic parameters: subplots from (a) to (f) are respectively for the shape parameter m and the scaling parameter U, the attenuation coefficient slope (ACS), the integrated backscattering coefficient (IBS), the effective acoustic concentration (EAC) and the effective scatterer diameter (ESD).

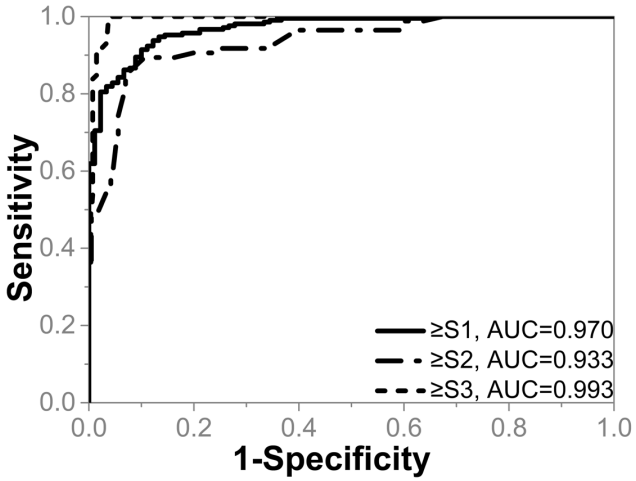

Figure 7. ROC curve corresponding to the merged characteristic parameters.

4. Discussions

Liver fatty deposits not only cause damage to liver tissue, but also cause lesions in other tissues. Studies have shown that NAFLD is more than just a liver disease, it is can also aggravate the incidence of diabetes and cardiovascular diseases [30]. Moreover, quantitative assessment of donor hepatic steatosis is critical in liver transplantation for the success of surgery [31, 32]. Therefore, it is of great clinical importance to accurately assess of the severity of NAFLD.

Various QUS parameters have been developed in previous studies for the NAFLD diagnosis. These parameters can assess the hepatic fat quantification from different aspects. How to combine these parameters for improving the diagnosis performance is still challenging. A recent study explored a multiparametric approach by combining QUS parameters to test the discriminate performance between the stages of liver fibrosis [33]. Linear discriminant analysis was used in that study for combining multiple parameters. This study applied a different combination method which is based on the criteria of maximizing the AUROC. The AUROC is used extensively in research to express discriminating power and diagnostic performance. Therefore, the combination method used in this study has unique advantage. It has the greatest AUROC out of all the possible linear combinations, ensuring that the performance of the combination is better than that of any individual method.

As shown Table 1, the four QUS parameters have different performances in distinguishing different steatosis stages. For distinguishing $\geq$ S1, $\geq$ S2, and =S3, IBC, m, EAC have the greatest AUROCs, respectively. Therefore, there is no one single parameter that is completely better than other parameters. The combination method can extract complementary information from different parameters compensate for the lack of a single characteristic parameter. It can be observed that the combination parameter has the highest AUROC than those of any single parameter for distinguishing $\geq$ S1. For other stages, although the combination parameter cannot achieve the highest AUROC compared with single parameter, it can improve the overall performance.

One limitation of our study comes from the animal model. The effectiveness of the proposed method was demonstrated using the NAFLD rat model. Its performance on human subjects need to be further tested through extra experiments. It would have been ideal to recruit clinical patients who have only varying levels of steatosis severity. However, this was a challenging task because steatosis, inflammation and fibrosis may precede or develop in parallel with the liver disease. Animal models of the spectrum of NAFLD provide the necessary tools to overcome confounding variables, such as genetic heterogeneity, and environmental factors, including diet and lifestyle. Given the difficulty of studying all the factors involved in steatosis in human populations, the animal model may have helped to improve our understanding of the physiopathology of the disease. Another limitation of the study is that ultrasonography was examined in ex vivo samples. In our study, we conducted ex-vivo liver experiments in order to isolate the liver fat factor from the confounding environment experienced in vivo experiments, so that the problem for NALFD can be examined independently. For the assessment of in vivo livers, other factors such as heart beat and blood flow must be considered as well. It could be recognized that the examination of the individual fat factor in ex-vivo livers can provide useful reference information for relevant studies in the in vivo experiments, as the QUS technique explores the microstructures of livers, the changes of which from in vivo to ex vivo are limited. In our future work, we shall deliver more efforts to extent the proposed technique to assess in vivo livers in rats and humans by taking the confounding environment into account. In addition, our work did not include comparisons

between quantitative US or their combined parameters and the standard ultrasound techniques utilized clinically. Adding relevant comparisons may provide more comprehensive interpretation of the results. Moreover, it should be noted that quantification of liver fat based on the US technique is one way to assess liver disease in NAFLD. However, liver inflammation cannot be measured with US. Fibrosis is the strongest and most relevant indicator of disease progression and can be more accurately quantified via biopsy and elastography [34].

5. Conclusion

We have proposed a multiparametric approach to explore the QUS parameters to differentiate between different steatosis stages. The findings show that this approach can make up for the deficiency of single parameter and improve the quantitative staging ability of fatty liver, and thus could play an important role in the diagnosis of NAFLD.

Acknowledgments

This work was supported by the National Natural Science Foundation of China (Grant Nos. 81871429 and 61427806), the Science and Technology Planning Project of Guangdong Province (No. 2017A020215099) and Shenzhen Science and Technology Planning Project (Grant No. JCYJ20160520175319943). We would like to thank the anonymous reviewers for their constructive comments and valuable suggestions.

Conflict of interest

The authors declare that there is no conflict of interests regarding the publication of this article.

References

1. P. Angulo, Nonalcoholic Fatty Liver Disease, *New Engl. J. Med.*, **346** (2002), 1221–1231.
2. G. C. Farrell and C. Z. Larter, Nonalcoholic fatty liver disease: From steatosis to cirrhosis, *Hepatology*, **43** (2006), S99–S112.
3. G. Targher, C. P. Day and E. Bonora, Risk of Cardiovascular Disease in Patients with Nonalcoholic Fatty Liver Disease, *New Engl. J. Med.*, **363** (2010), 1341–1350.
4. Y. Takahashi and T. Fukusato, Histopathology of nonalcoholic fatty liver disease/nonalcoholic steatohepatitis, *World J. Gastroenterol.*, **20** (2014), 15539–15548.
5. N. Zamcheck and R. L. Sidman, Needle biopsy of the liver. I. Its use in clinical and investigative medicine, *New Engl. J. Med.*, **249** (1953), 1020–1029.
6. Y. Sumida, A. Nakajima and Y. Itoh, Limitations of liver biopsy and non-invasive diagnostic tests for the diagnosis of nonalcoholic fatty liver disease/nonalcoholic steatohepatitis, *World J. Gastroenterol.*, **20** (2014), 475-485.
7. N. F. Schwenzer, F. Springer, C. Schraml, et al., Non-invasive assessment and quantification of liver steatosis by ultrasound, computed tomography and magnetic resonance, *J. Hepatol.*, **51** (2009), 433-445.

8. S. B. Reeder, I. Cruite, G. Hamilton, et al., Quantitative Assessment of Liver Fat with Magnetic Resonance Imaging and Spectroscopy, *J. Magn. Reson. Imaging*, **34** (2011), 729–749.
9. S. Saadeh, Z. M. Younossi, E. M. Remer, et al., The utility of radiological imaging in nonalcoholic fatty liver disease, *Gastroenterology*, **123** (2002), 745–750.
10. Y. Guo, C. Dong, H. Lin, et al., Evaluation of Non-alcoholic Fatty Liver Disease Using Acoustic Radiation Force Impulse Imaging Elastography in Rat Models, *Ultrasound Med. Biol.*, **43** (2017), 2619–2628.
11. C. D. Williams, J. Stengel, M. I. Asike, et al., Prevalence of Nonalcoholic Fatty Liver Disease and Nonalcoholic Steatohepatitis Among a Largely Middle-Aged Population Utilizing Ultrasound and Liver Biopsy: A Prospective Study, *Gastroenterology*, **140** (2011), 124–131.
12. A. E. Bohte, J. R. van Werven, S. Bipat, et al., The diagnostic accuracy of US, CT, MRI and 1 H-MRS for the evaluation of hepatic steatosis compared with liver biopsy: a meta-analysis, *Eur. Radiol.*, **21** (2011), 87–97.
13. A. Ozturk, J. R. Grajo, M. S. Gee, et al., Quantitative hepatic fat quantification in non-alcoholic fatty liver disease using ultrasound-based techniques: A review of literature and their diagnostic performance, *Ultrasound Med. Biol.*, **44** (2018), 2461–2475.
14. M. L. Oelze and J. Mamou, Review of Quantitative Ultrasound: Envelope Statistics and Backscatter Coefficient Imaging and Contributions to Diagnostic Ultrasound, *IEEE Transa. Ultrason., Ferroelectr. Freq. Control*, **63** (2016), 336–351.
15. F. Destrempes and G. Cloutier, A critical review and uniformized representation of statistical distributions modeling the ultrasound echo envelope, *Ultrasound Med. Biol.*, **36** (2010), 1037–1051.
16. M. C. Ho, Y. H. Lee, Y. M. Jeng, et al., Relationship between Ultrasound Backscattered Statistics and the Concentration of Fatty Droplets in Livers: An Animal Study, *PloS One*, **8** (2013), e63543.
17. P. H. Tsui and Y. L. Wan, Application of Ultrasound Nakagami Imaging for the Diagnosis of Fatty Liver, *J. Med. Ultrasound*, **24** (2016), 47–49.
18. Y. L. Wan, D. I. Tai, H. Y. Ma, et al., Effects of fatty infiltration in human livers on the backscattered statistics of ultrasound imaging, *Proc. Inst. Mech. Eng. Part H-J. Eng. Med.*, **229** (2015), 419–428.
19. J. S. Paige, G. S. Bernstein, E. Heba, et al., A Pilot Comparative Study of Quantitative Ultrasound, Conventional Ultrasound, and MRI for Predicting Histology-Determined Steatosis Grade in Adult Nonalcoholic Fatty Liver Disease, *Am. J. Roentgenol.*, **207** (2017), W168–W177.
20. H. T. Yang, K. F. Chen, Q. Lu, et al., Ultrasonic integrated backscatter in assessing liver steatosis before and after liver transplantation, *Hepatobiliary Pancreatic Dis. Int.*, **13** (2014), 402–408.
21. S. C. Lin, E. Heba, T. Wolfson, et al., Noninvasive Diagnosis of Nonalcoholic Fatty Liver Disease and Quantification of Liver Fat Using a New Quantitative Ultrasound Technique, *Clin. Gastroenterol. Hepatol.*, **13** (2015), 1337–1345.
22. G. Ghoshal, R. J. Lavarello, J. P. Kemmerer, et al., Ex vivo study of quantitative ultrasound parameters in fatty rabbit livers, *Ultrasound Med. Biol.*, **38** (2012), 2238–2248.

23. D. E. Kleiner, E. M. Brunt, M. Van Natta, et al., Design and validation of a histological scoring system for nonalcoholic fatty liver disease, *Hepatology*, **41** (2005), 1313–1321.

24. J. J. Lin, J. Y. Cheng, L. F. Huang, et al., Detecting changes in ultrasound backscattered statistics by using Nakagami parameters: Comparisons of moment-based and maximum likelihood estimators, *Ultrasonics*, **77** (2017), 133–143.

25. K. Samimi and T. Varghese, Ultrasonic attenuation imaging using spectral cross-correlation and the reference phantom method, *2011 IEEE Int. Ultrason. Symp.*, (2011), 53–55.

26. V. Roberjot, S. L. Bridal, P. Laugier, et al., Absolute backscatter coefficient over a wide range of frequencies in a tissue mimicking phantom containing two populations of scatterers, *IEEE Trans. Ultrason., Ferroelectr. Freq. Control*, **43** (1996), 970–978.

27. F. L. Lizzi, M. Astor, L. Tian, et al., Ultrasonic spectrum analysis for tissue assays and therapy evaluation, *Int. J. Imaging Syst. Technol.*, **8** (1997), 3–10.

28. J. Q. Su and J. S. Liu, Linear Combinations of Multiple Diagnostic Markers, *Publ. Am. Stat. Assoc.*, **88** (1993), 1350–1355.

29. Y. Liu, C. F. Dong, G. Yang, et al., Optimal linear combination of ARFI, transient elastography, and APRI for the assessment of fibrosis in chronic hepatitis B, *Liver Int.*, **35** (2015), 816–825.

30. S. Milić and D. Štimac, Nonalcoholic Fatty Liver Disease/Steatohepatitis: Epidemiology, Pathogenesis, Clinical Presentation and Treatment, *Dig. Dis.*, **30** (2012), 158–162.

31. C. D. Byrne and G. Targher, NAFLD: A multisystem disease, *J. Hepatol.*, **62** (2015), S47–S64.

32. R. J. Wong, M. Aguilar, P. Cheung, et al., Nonalcoholic Steatohepatitis Is the Second Leading Etiology of Liver Disease Among Adults Awaiting Liver Transplantation in the United States, *Gastroenterology*, **148** (2015), 547–555.

33. R. Bouzitoune, M. Meziri, C. B. Machado, et al., Can early hepatic fibrosis stages be discriminated by combining ultrasonic parameters?, *Ultrasonics*, **68** (2016), 120–126.

34. X. Chen, H. Wen, X. Zhang, et al., Development of a Simple Noninvasive Model to Predict Significant Fibrosis in Patients with Chronic Hepatitis B: Combination of Ultrasound Elastography, Serum Biomarkers, and Individual Characteristics, *Clin. Transl. Gastroenterol.*, **8** (2017), e84.

AIMS Press